FEM Numerical Model Analysis of Magnetic Nanoparticle Tumor Heating Experiments

John A. Pearce, *Life Senior Member, IEEE*, Alicia A. Petyk, and P. Jack Hoopes

***Abstract*—Iron oxide nanoparticles are currently under investigation as heating agents for hyperthermic treatment of tumors. Major determinants of effective heating include the biodistribution of magnetic materials, the minimum iron oxide loading required to achieve adequate heating, and practically achievable magnetic field strengths. These are inter-related criteria that ultimately determine the practicability of this approach to tumor treatment.**

Currently, we lack fundamental engineering design criteria that can be used in treatment planning and assessment. Coupling numerical models to experimental studies illuminate the underlying physical processes and can separate physical processes to determine their relative importance. Further, adding thermal damage and cell death process to the models provides valuable perspective on the likelihood of successful treatment. FEM numerical models were applied to increase the understanding of a carefully calibrated series of experiments in mouse mammary carcinoma. The numerical models results indicate that tumor loadings equivalent to approximately 1 mg of Fe_3O_4 per gram of tumor tissue are required to achieve adequate heating in magnetic field strengths of 34 kA/m (rms) at 160 kHz. Further, the models indicate that direct intra-tumoral injection of the nanoparticles results in between 1 and 20% uptake in the tissues.

I. Introduction

MAGNETIC nanoparticles, typically iron oxide (IONPs) in the form of Fe_3O_4 with some type of bio-compatible coating such as starch or polyethylene glycol, are under investigation for tumor treatment, either by direct thermal damage or as an adjunct for other therapies. Key to success in this application is obtaining adequate heat in the target tissues. It is well understood that tumor vasculature has larger inter-endothelial gaps than most normal tissues, and that cells will transport IONPs from the extracellular space and cluster them into intracellular endosomes. However, owing to their small size and the overwhelming influence of local heat transfer, it is not clear that an adequate tumor load of magnetic nanoparticle (mNP) absorbing material can be accumulated to provide sufficient power absorption in practical magnetic fields. At present, the required tumoral mNP loading has not been determined quantitatively. Additionally, the range of practically achievable tumor loading has not been determined to date.

We undertook a series of *in vivo* experiments coupled with realistic Finite Element Method (FEM) numerical models studies to determine quantitative values that could be used in treatment planning and assessment.

Manuscript received March xx, 2014. This work was supported in part by the T.L.L. Temple Foundation and by NIH NCI Grant No. 1U54CA151662-03.

J. A. Pearce is Temple Foundation Professor of Electrical and Computer Engineering at the University of Texas at Austin, 1 University Station, Austin, TX 78712. (telephone: 512-471-4984; fax: 512-471-3652; e-mail: jpearce@mail.utexas.edu).

Alicia Petryk is a Post-Doctoral Research Engineer in the Giesel School of Medicine at Dartmouth College.

P. Jack Hoopes is Professor of Medicine and of Engineering in the Giesel School of Medicine and Thayer School of Engineering, respectively, at Dartmouth College.

II. Methods

A. Experimental Studies

All animal experimentation was conducted under protocols approved by the Dartmouth IACUC in accordance with NIH guidelines.

Bilateral MTG-B tumors were implanted in the fore shoulders of six female C3H mice and allowed to develop for two weeks prior to treatment. Resulting tumor volumes ranged from 250 to 508 mm^3 at the time of treatment. The mouse fore shoulders were exposed to magnetic fields of approximately 34 kA/m (rms) at 160 kHz for heating times between 300 and 3,600 s (5 to 60 min.). Transient intra-tumoral, rectal and skin surface temperatures, as well as at several nearby points were recorded at 1s intervals using FISO optical probes 0.56 mm in diameter (FISO Inc., Quebec, Canada). The real-time skin surface temperature was also recorded with a FLIR Systems (Wilsonville,OR) thermal camera.

At the conclusion of the experiment the animals were euthanized, tumor tissues were excised and submitted for histologic evaluation.

B. Numerical Model Studies

FEM numerical models were constructed and executed in Comsol (Comsol, Inc. Burlington MA). Tumors were represented by ellipsoids based on the measured tumor dimensions for the individual experiments. The models assumed an equivalent uniform volumetric heating, and the volume power generation term in the Bioheat Equation, Q_{gen} (W/m^3):

$$\rho_t c_t \frac{\partial T}{\partial t} = \nabla \bullet \left(k \nabla T \right) + Q_{gen} + Q_{met} + \dot{w} \rho_t c_b \left[T - T_a \right] \quad (1)$$

where: ρ_t = tissue density, c = specific heat, k = thermal conductivity, Q_{met} = metabolic heat (W/m^3), w = perfusion (s^{-1}) and T = temperature (see Table I). Q_{gen} was adjusted until the experiment transient temperature record was closely approximated by the numerical model result.

Table I
Thermal Model Parameters

Tissue	k	ρ	c	Q_{met}	w
Skin	0.3	700	3700	250	0.88×10^{-3}
Muscle	0.5	1050	3700	1000	1.75×10^{-3}
Tumor	0.4	900	3700	1300	1.75×10^{-3}
Blood		1050	4186		

Volumetric heating in the iron oxide nanoparticles is dominated by Neél relaxation processes in the net magnetic spin moments at 160 kHz, denoted by the imaginary part of the magnetic permeability, μ" (Hy/m):

$$Q_{gen} = \omega \mu'' \left|\mathbf{H}\right|^2 \qquad (2)$$

where: ω = the angular frequency (r/s), and **H** = the vector magnetic field strength (A/m). The relaxation phenomenon appears as an opening in the **B**-**H** hysteresis loop, where **B** = the magnetic flux density (T). For the BNF-starch mNPs (MicroMod, 100-00-102, MicroMod Partikeltechnologie, Gmbh, Rostock, Germany) used in this study the hysteresis loop is maximally open at about 14 (kA/m) rms, where the relative μ" = 6, as in Fig. 1.

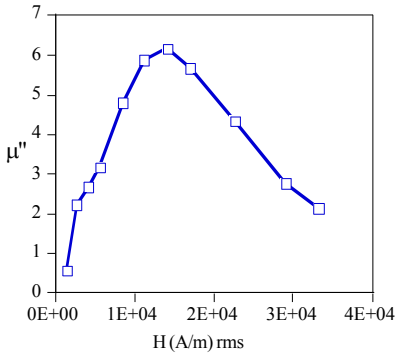

Fig. 1 Imaginary part of the relative magnetic permeability is maximal at about 14 (kA/m) at 150 kHz.[1]

The experiments were conducted at 162 kHz in a field strength of approximately 34 (kA/m rms) where the relative μ" ≃ 3, so the maximum achievable volumetric power density in the iron oxide was approximately 9×10^9 (W/m^3). The magnetic material sizes range from hydrodynamic diameters of 60 to 120 nm and the Fe_3O_4 occupies between 30 and 43% of the nanoparticle volume and only a very small fraction of the total tumor volume in each experiment.

The effective tumor loading of the injected nanoparticles cannot be determined by experimental means alone. The numerical model results were therefore used to estimate the tumor loading achieved in each of the experiments by comparing the uniform Q_{gen} required to model the temperature record with the maximum achievable heating assuming 100% uptake in the tumor.

The numerical models also included three thermal damage predictions, microvascular damage[2], Dunning AT-1 cell death, as measured by histologic identification of apoptosis and necrosis[3], and SN12 cell death as measured by propidium iodide uptake in damaged cells.[4] The damage model was calculated from Arrhenius kinetics:

$$\Omega(\tau) = ln\left\{\frac{C(0)}{C(\tau)}\right\} = \int_0^\tau A\, e^{\left[\frac{-E_a}{R\,T(t)}\right]}\, dt \qquad (3a)$$

$$C(\tau) = e^{-\Omega} \qquad (3b)$$

where: C(t) = the remaining undamaged fraction, τ = total experiment time (s), T = temperature (K), E_a = the activation energy (J/mole), and A = the frequency factor (s^{-1}) for the damage process (Table II).

Table II
Damage Process Parameters

Process	E_a (J/mole)	A (s^{-1})
Microvascular damage	6.67×10^5	1.98×10^{106}
AT-1 cell death	5.68×10^5	1.66×10^{91}
SN12 cell death	2.88×10^5	4.46×10^{43}

III. Results

A. Transient Temperature Results

Experiment heating times ranged from 300 to 3600 (s) and maximum temperatures from 39 to 57 C. The experiment in Fig. 2 was the shortest in the ensemble, and achieved 51 C after 300 s of heating. Steady state had not been reached at the conclusion (Fig. 2a). The numerical model (Fig. 2b) provided a reasonable match at $Q_{gen} = 1 \times 10^6$ (W/m^3). In the numerical model 600 s were allowed to reach the resting steady state before heating commenced. The particular tumor had ellipsiodal diameter dimensions of 11, 8.5 and 6.3 (height) mm (volume = 307 mm^3). The estimated maximum volume average power generation at 34 (kA/m) was 6.2 (MW/m^3). Consequently, we estimate an overall coupling efficiency of about 16% for this experiment: that is, the biodistribution realized was about 16% of the injected mass of iron oxide nanoparticles resident in the tumor at experiment time.

The top skin surface was a convective heat transfer boundary with convection coefficient h = 20 ($W\ m^{-2}\ K^{-1}$). The skin temperature of approximately 32 C at the end of the cooling phase agreed well with the experimental measurements. The temperature over the tumor was slightly

higher than the surrounding skin due to the slightly higher metabolic heat (Table I). The second phase, tumor heating, applied Q_{gen} for the heating duration, and 200 s of cooling followed. The cooling transient temperature record matched the experiment with acceptable accuracy (Fig. 2), indicating that the assumed heat transfer parameters were reasonable.

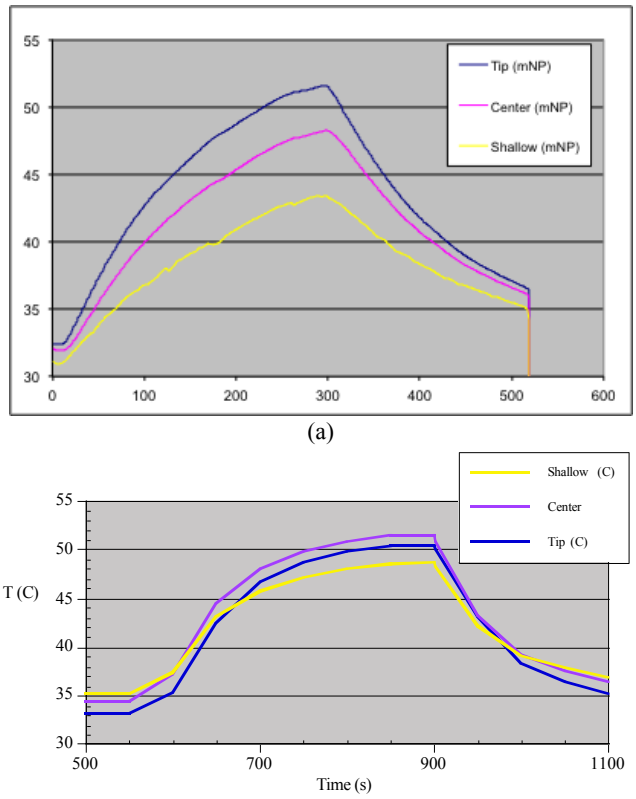

Fig. 2 a) Measured transient temperatures on the embedded optical temperature linear probe at "shallow", "center" and "tip" locations. The maximum temperature near the tumor center was 48 C in the experiment. b) FEM numerical model transient temperatures at similar locations in the simulated tumor. Here the maximum temperature on the model tumor reached 51 C.

As is the usual case, there are several differences between experiment and numerical model. For example, in Fig. 2 the temperature probe locations were estimated in the numerical model, and differed in either effective spatial location, or local biodistribution of mNPs. In all of the experiments, the magnetic field strength was kept constant. Two of the experiments showed evidence of vascular shutdown — a rapid temperature increase in the final stage of heating — that was not observed in the numerical models in spite of coupling the microvascular damage process to the local perfusion. One example is shown in Fig. 3a, wherein the final maximum tumor temperature, 54 C, only occurred in the final few seconds of heating. The numerical model, Fig. 3b, did not have an analogous spike in the final result. Consequently, the thermal damage predictions for that model likely under estimate the *in vivo* result.

B. Thermal Damage and Cell Death Predictions

As may be surmised from the Arhenius damage model coefficients in Table II, the SN12 cells are much more thermally-robust than the AT-1 cells. The numerical model results (Table III) bear this out. The kinetic nature of the damage process development is also evident in the differences between microvascular damage and AT-1 cell death in experiments of differing heating durations. The apparent anomaly in the sequencing of the damage predictions in Table III is explained by the temperature spike in the higher temperature experiment contrasted with the absence of the spike in the associated numerical model, as previously mentioned

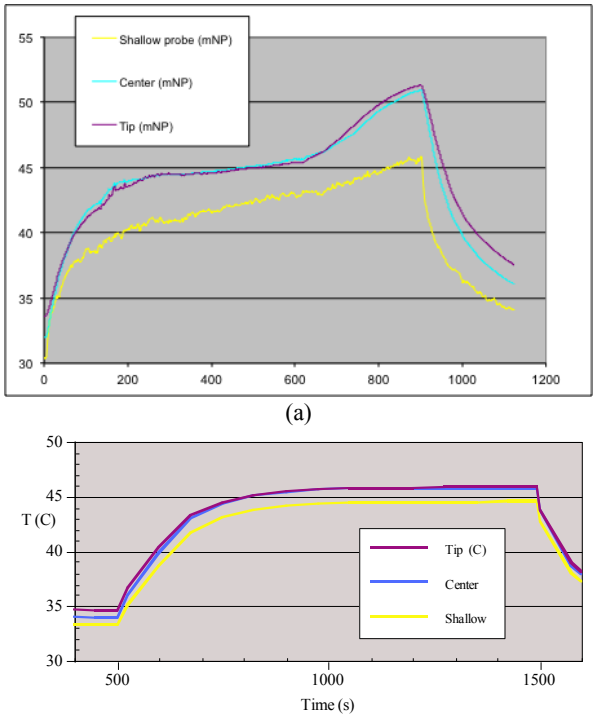

Fig. 3 a) Measured transient temperatures (T_{max} = 51 C) and b) FEM numerical model transient temperatures (T_{max} = 46 C). The late term spike in the experiment is evidence of vascular shutdown not successfully modeled.

Table III
FEM Model Thermal Damage and Cell Death Predictions

T_{max} Tumor Center (C)	Heating Time (s)	Micro-Vascular Damage (%)	~ % Tumor Vol.	AT-1 Cell Death (%)	~ % Tumor Vol.	Max. SN12 Cell Death
57	600	100	100	100	100	73
54	1300	100	100	100	100	89
51*	900	59		100	80	6.7
48	300	100	50	100	90	12
40	3600	7.2		83		4.6
39	1800	Not Modeled				

* a temperature spike in this experiment (Fig. 3a) that was not successfully modeled (Fig. 3b) explains the anomalous sequence in damage predictions.

C. Estimates of Effective mNP Loading for the Experiments

FEM numerical model volume average power densities (Q_{gen}) were selected to provide the best match to the steady state final temperatures in order to provide an estimate of the effective power coupled to tumor tissue. The anomaly described in Fig. 3 resulted from this selection criterion.

The maximum power coupled to the tumor was estimated from the injected mass of iron oxide nanoparticles using Eq. (2) and an iron oxide density of 5242 (kg/m^3). The experiment series was designed around an assumed achievable average volume power density of approximately 6 (MW/m^3) with the exception of one experiment (see Table IV). The uniform volume power density required to simulate the experiment was used to estimate the probable overall effective power coupling efficiency, which ranged from less than 3 to approximately 20%. The results summarized in Table IV are listed in sequence of the maximum experimental temperature, the same sequence as Table III. The estimated effective tumor loading ranged from 0.5 to 1.5 μg/mm^3, or approximately 0.48 to 0.14 mg/g of tumor. There are several sources of uncertainty in the estimates due to: 1) variations in net tumor uptake, 2) spatial distribution of the mNPs in the tumor, 3) variations in the applied magnetic field due to positioning above the pancake coil. The overall estimate calculations assume: 1) a uniform mNP distribution, and 2) a uniform magnetic field strength for all experiments. Consequently, the overall coupling estimate below lumps all uncertainties into a net tumor uptake estimate.

Table IV
Mouse Experiment and FEM Numerical Model Results

Experiment					Numerical Model		
Tumor Vol. (μL)	Fe_3O_4 (mg)	P_{tot} (W)	Q_{gen} Max (MW/m^3)	T_{max} (C)	Q_{gen} Model (MW/m^3)	Eff. (%)	Estimated Tumor Load (μg/mm^3)
329	2.45	4.04	6.1	57	1.2	19.7	1.47
508	3.81	6.3	6.2	54	0.9	14.8	1.11
310	2.33	3.84	6.1	51	0.6	10.2	0.77
307	2.3	3.8	6.2	48	1	16	1.2
250	4.62	7.62	15.3	40	0.43	2.8	0.5
302	2.27	3.75	6.1	39	Not Modeled		

IV. Conclusion

The numerical model study has significantly improved our understanding of the experiment series and identified several important underlying phenomena. The near-surface locations and small size of tumors in this experiment ensemble mean that surface heat transfer is a governing thermal phenomenon: most of the experiments resulted in steady-state temperature rises in which Q_{gen} was balanced by local heat transfer. Successful heating of near surface tumors in the size range of 5 to 10 mm requires an effective tumor loading in excess of approximately 1 μg/mm^3 (about 0.9 mg/g tumor). This is a significant treatment design parameter that establishes a useful treatment-planning criterion for mNP biodistribution. The results also reveal the differing nature of "success" as measured by thermal damage kinetics. That is, a single assessment criterion, such as CEM_{43}, can be substantially misleading since it masks the differences among cell types and the kinetics of their responses to thermal insult. Realistic treatment planning must incorporate some analysis of the range of responses to be expected and the effect of varying kinetics.

References

[1] J.A. Pearce, A.J. Giustini, R. Stigliano, and P.J. Hoopes, "Magnetic Heating of Nanoparticles: The Importance of Particle Clustering to Achieve Therapeutic Temperatures," *Journal of Nanotechnology in Engineering and Medicine*, vol. 4, (no. 1), pp. 011005, 2013.

[2] S.L. Brown, J.W. Hunt, and R.P. Hill, "Differential thermal sensitivity of tumour and normal tissue microvascular response during hyperthermia," *International Journal of Hyperthermia*, vol. 8, pp. 501-504, 1992.

[3] S. Bhowmick, D.J. Swanlund, and J.C. Bischof, "In vitro thermal therapy of AT-1 Dunning prostate tumours," *International Journal of Hyperthermia*, vol. 20, (no. 1), pp. 73–92, 2004.

[4] X. He and J.C. Bischof, "The Kinetics of Thermal Injury in Human Renal Carcinoma Cells," *Annals of Biomedical Engineering*, vol. 33, (no. 4), pp. 502-510, 2005.